Chemical Science

EDGE ARTICLE

View Article Online
View Journal | View Issue

Cite this: *Chem. Sci.*, 2017, **8**, 3494

p-Doping of graphene in hybrid materials with 3,10-diazapicenium dications†

Alexandra Roth,‡[a] Tobias A. Schaub,‡[b] Ute Meinhardt,[b] Dominik Thiel,[a] Jan Storch,[c] Vladimír Církva,[c] Pavel Jakubík,[c] Dirk M. Guldi*[a] and Milan Kivala*[b]

Received 4th February 2017
Accepted 22nd February 2017

DOI: 10.1039/c7sc00533d

rsc.li/chemical-science

N,*N*′-Didodecyl-substituted 3,10-diazapicenium salts featuring bromide and hexafluorophosphate counterions have been designed as novel dopants to realize individualized graphene sheets in a series of cutting edge experiments and to intrinsically stabilize them *via* p-doping. Importantly, electrochemical studies revealed two consecutive irreversible one-electron reductions of the *N*,*N*′-didodecyl-substituted 3,10-diazapicenium salts to yield the corresponding radical cation and neutral quinoidal species. Formation of both species was accompanied by characteristic changes in the absorption spectra. The 3,10-diazapicenium bromide was found to be a potent dopant to produce hybrid materials with exfoliated graphene. Microscopy based on AFM and TEM imaging and spectroscopy based on Raman probing corroborated that, upon drying, the hybrid material consists of few layer (5–8 layers) turbostratic graphene sheets that are p-doped. Our findings identify the newly synthesized *N*,*N*′-dialkylated 3,10-diazapicenium salts as highly promising candidates for the fabrication of functional graphene materials with tailored properties.

Introduction

Hybrid systems featuring π-conjugated molecular building blocks and exfoliated graphite hold enormous promises for various applications due to the possibility to modulate the electronic nature of the graphene flakes.[1] Since its seminal realization, graphene and its production methods have been at the forefront of multidisciplinary studies aiming at its application in, for example, next generation organic electronic devices.[2,3] In general, graphene is prepared by either physical[4] or chemical processes,[5] whereby its quantity and quality decisively impacts the development and performance of prospective applications.[3] The liquid phase exfoliation of graphite represents a particularly appealing strategy as it opens up new avenues to construct unprecedented hybrid systems.[6] Even though this approach still poses myriads of challenges, hybrid materials consisting of functionalized polycyclic aromatic scaffolds and (nano)graphene came to the forefront in recent years.[7–9] Overall, the degree of individualization is controlled by the nature of the molecular exfoliant–the use of planar and rigid scaffolds including porphyrins,[7,10] phthalocyanines,[11] or perylene-3,4,9,10-tetracarboxylic dianhydrides[12] amongst others turned out to be particularly effective for graphite exfoliation. Depending on the electron-deficient or -rich nature of the exfoliant, the liquid phase delamination of graphite represents a versatile methodology to produce p- or n-type doped (nano)graphene hybrids, respectively. The more so, as the careful chemical modification of the molecular exfoliant enables precise control over the degree of doping.[13] Through this approach graphene flakes with tailored electronic properties are in reach and the scope of potential applications of graphene in nanoelectronics seems sheer endless.[14]

To the best of our knowledge, apart from the previous report by Stoddart *et al.*,[15] who employed 2,9-diazaperopyrenium dication **A** to directly exfoliate graphite in aqueous media (Fig. 1), positively charged polycyclic aromatic exfoliants have never been utilized. As a matter of fact, it has been documented that the comparatively small size of 2,7-diazapyrenium dication **B** is insufficient for an intercalation between graphite layers and, in turn, exfoliation of single graphene flakes from graphite.[15] A careful consideration of structural prerequisites such as rigidity and planarity of an extended π-conjugation paired with inherent redox activity prompted us to design and realize *N*,*N*′-dialkylated 3,10-diazapicenium dication **C**. As such, dication **C** combines the features of an exfoliant, a stabilizer, and a p-dopant.

[a]*Institute for Physical Chemistry I, Department Chemistry and Pharmacy, University of Erlangen-Nürnberg, Egerlandstrasse 3, D-91058 Erlangen, Germany. E-mail: dirk.guldi@fau.de*

[b]*Institute for Organic Chemistry I, Department of Chemistry and Pharmacy, University of Erlangen-Nürnberg, Henkestrasse 42, D-91054 Erlangen, Germany. E-mail: milan.kivala@fau.de*

[c]*Institute of Chemical Process Fundamentals of the Czech Academy of Sciences, Rozvojová 135/1, CZ-165 02 Prague 6, Czech Republic*

† Electronic supplementary information (ESI) available: Synthetic details and additional spectra. See DOI: 10.1039/c7sc00533d

‡ These authors contributed equally.

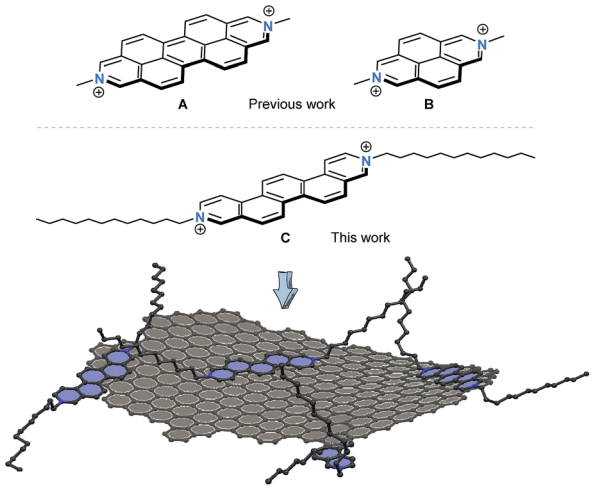

Fig. 1 Chemical structures of dications A and B studied previously by Stoddart *et al.*[15] as exfoliating agents for graphite. Chemical structure of the 3,10-diazapicenium dication C examined in this work. Schematic illustration of a graphene flake stabilized by the diazapicenium dications – counterions are omitted for the sake of simplicity.

Results and discussion

Synthesis and photophysical characterization of *N*,*N*′-dialkyl-3,10-diazapicenium salts

The parent 3,10-diazapicene scaffold **1**, a member of the hitherto rather underrepresented family of hetero[*n*]-phenacenes,[16] was accessible through microwave-assisted photocyclization of the corresponding diazastilbenes.[17] To enhance the solubility of **1** [18] and to introduce electron-accepting properties, *n*-dodecyl alkyl chains were introduced at the pyridyl nitrogens (for synthetic details, see ESI†). In analogy to the reaction conditions optimized for the dialkylation of related 4,4′-bipyridines, so-called viologens,[19] reaction of **1** with 1-bromododecane at 130 °C in *N*,*N*-dimethylformamide (DMF) under microwave irradiation furnished the *N*,*N*′-didodecyl decorated 3,10-diazapicenium dibromide salt **2** in 89% yield (Scheme 1). To study the impact of the counterion on the photophysical and electrochemical properties, anion exchange reactions were carried out. For that purpose, addition of ammonium hexafluorophosphate to a solution of dibromide **2** in an EtOH/H_2O mixture resulted in nearly quantitative precipitation of 3,10-diazapicenium bis(hexafluorophosphate) **3**. Compounds **2** and **3** were isolated as air stable, yellow powders, which show sufficient solubility in common organic solvents.

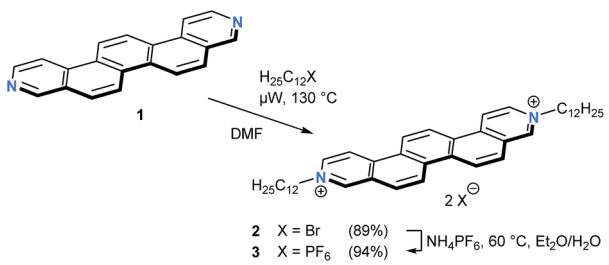

Scheme 1 Synthesis of the *N*,*N*′-dialkylated 3,10-diazapicenium dications.

To gain insights into the characteristics of 3,10-diazapicene **1** and its dialkylated salts **2** and **3**, absorption and fluorescence studies were performed in EtOH (Fig. 2). Strong absorptions in the UV region (240–340 nm for **1**, 250–350 nm for **2** and **3**) followed by weak absorptions centered in the visible region (340–390 nm for **1**, 370–440 nm for **2** and **3**) were observed due to $S_0 \rightarrow S_2$ and $S_0 \rightarrow S_1$ transitions, respectively.[20] The vibrational fine structure with a spacing in the range from 1350 to 1430 cm^{-1} stems from several in-plane C–H bending and ring breathing modes as previously reported for picene[20] and smaller rigid viologens.[21] Upon dialkylation of **1**, the spectroscopic features are bathochromically shifted by about 42 nm for **2** and **3** and are independent on the nature of the counterion. Energies of the fundamental $S_0 \rightarrow S_1$ transitions were estimated as 3.18, 2.79, and 2.77 eV for **1**, **2** and **3**, respectively, (Table 1).

Compounds **1**, **2**, and **3** exhibit intense blue fluorescence in EtOH. For example, the fluorescence of 3,10-diazapicene **1** maximizes at 386, 408, 432, and 459 nm. In contrast, the fluorescence of **2** and **3** is far less resolved with a maximum centered at 442 nm and a shoulder at 464 nm. All compounds **1–3** feature similar fluorescence quantum yields with 0.21–0.22 and Stokes shifts of 910 cm^{-1}. The excitation spectra of **1–3** closely resemble their absorption spectra and, thus, confirm their monomeric nature. These results clearly show that the

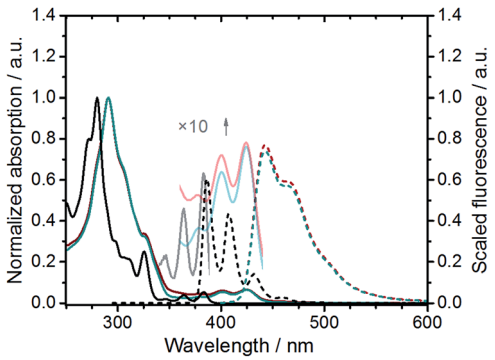

Fig. 2 Normalized absorption (solid lines) and fluorescence spectra (dashed lines) of **1** (black, $\lambda_{exc} = 324$ nm), **2** (blue, $\lambda_{exc} = 390$ nm), and **3** (red, $\lambda_{exc} = 390$ nm) in EtOH.

Table 1 Selected photophysical and cyclic voltammetry data of compounds **1–3**

	λ_{max} [a]/nm	E_{gap} [b]/eV	λ_{em} [c]/nm (ϕ/a.u.)	τ [d]/ns	$E_{red,1}$ [e] ($E_{red,2}$)/V
1	383	3.18	386	n/a	n/a
2	426	2.79	443 (0.22)	11.4	−1.10 (−1.52)
3	425	2.77	442 (0.22)	10.7	−1.10 (−1.51)

[a] Measured in EtOH. [b] Band gap calculated from onset of the absorption at $0.1\lambda_{max}$. [c] Fluorescence quantum yields measured in EtOH with Coumarin 47 as reference ($\phi_{ref} = 0.73$).[25] [d] Fluorescence lifetimes from TCSPC measurements ($\lambda_{exc} = 403$ nm). [e] Half-wave potentials recorded by cyclic voltammetry in CH_2Cl_2 with 0.1 M nBu_4NPF_6 (scan rate 200 mV s^{-1}, referenced *vs.* Fc/Fc^+).

spectroscopic features of *N*,*N*′-dialkylated 3,10-diazapicenium dications are not impacted by the counterion pointing to the presence of solvent separated ion pairs in solution.[22] The fluorescence spectra are reasonable mirror images of the absorption spectra including vibrational fine structure indicative of a rigid aromatic fluorophore.[21]

To determine the fluorescence lifetimes, time-correlated-single-photon-counting (TCSPC) measurements were performed in EtOH with an excitation wavelength of 403 nm and the resulting decays were fit by a monoexponential fitting function. We find that the bromide salt **2** and the hexafluorophosphate salt **3** display comparable fluorescence lifetimes of 11.4 and 10.7 ns (Table 1).

The characterization of diazapicenium bromide **2** was complemented by femtosecond transient absorption spectroscopy to gather a deeper insight into the excited state features and their dynamics. The deconvoluted transient absorption spectra for **2** in EtOH upon excitation at 387 nm taken from a global analysis are shown in Fig. 3 together with the time–concentration profiles. To this end, the singlet excited state features were found in the visible as well as in the near infrared region with maxima at 455, 480, 630, 920, and 1035 nm. All of them are formed instantaneously upon excitation and feature a lifetime of 9.7 ± 1.0 ns. The corresponding intersystem crossing produces a triplet excited state, whose lifetime is 280 ± 30 ns, and whose signature is a 615 nm maximum.

To evaluate the electron accepting strength of **2** and **3**, their electrochemical properties were examined by means of cyclic voltammetry in CH_2Cl_2 with 0.1 M nBu$_4$NPF$_6$ as a supporting electrolyte at a scan rate of 200 mV s^{-1}. Glassy carbon served as a working electrode, a platinum wire as counter electrode, and a Ag/AgCl as pseudo-reference electrode. Overall, the redox properties, which are independent on the nature of the counterions, give rise to two irreversible one-electron reductions at −1.10 V *vs.* Fc/Fc$^+$ (E_{LUMO} = −3.7 eV)[23] and −1.51 V *vs.* Fc/Fc$^+$ for **2** and **3** (Table 1, see ESI†). Both reductions to afford the corresponding radical cation and subsequently neutral quinoidal form of the *N*,*N*′-dialkylated 3,10-diazapicenium salts are comparable to those reported for *N*,*N*′-dialkylated 3,8-diazaphenanthrenium viologens and related compounds (Fig. 4).[21,24] Notably, the first reduction of **2** and **3** is within the range of electron-deficient aromatics as previously used to fabricate non-covalently p-type doped graphene hybrid materials.[7,9,11]

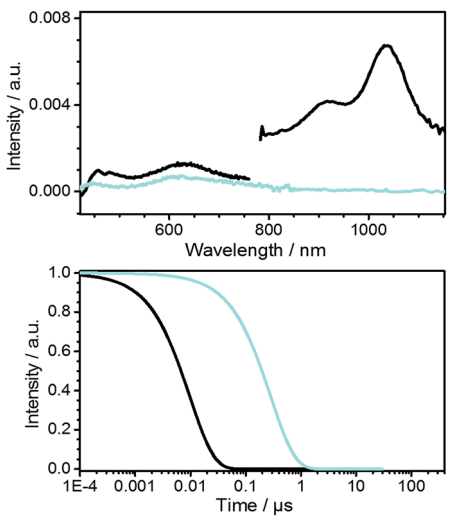

Fig. 3 Top: deconvoluted transient absorption spectra of the singlet (black) and triplet (cyan) excited state of **2** in EtOH obtained by global analysis. Bottom: corresponding concentration–time profiles.

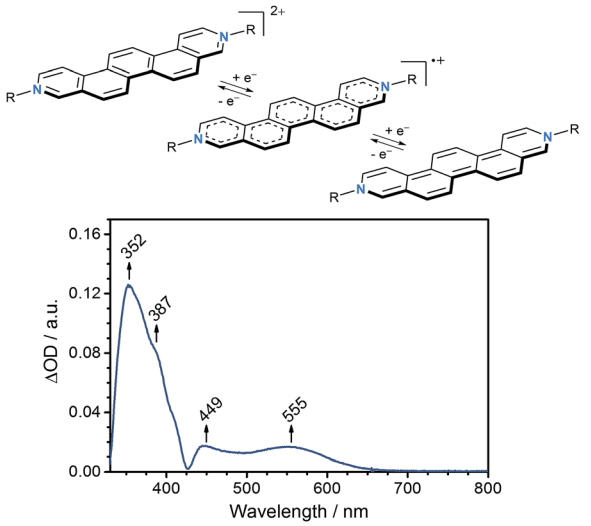

Fig. 4 Top: two one-electron reductions of *N*,*N*′-dialkylated 3,10-diazapicenium salts (R = alkyl); bottom: differential absorption spectrum of **2** in dry DMF obtained by subtracting the absorption spectrum of **2** recorded at 0.0 V from that recorded at −0.7 V *vs.* Ag wire.

Based on these results, spectroelectrochemical studies were performed for **2** in dry DMF containing 0.1 M nBu$_4$NPF$_6$ as supporting electrolyte. As working electrode, a platinum mesh was used, while the counter electrode was a platinum plate and a silver wire was used as reference electrode. In agreement with the findings from cyclic voltammetry, the differential absorption spectrum recorded at −0.70 V *vs.* Ag wire (*ca.* −1.10 V *vs.* Fc/Fc$^+$)[26] reveals characteristic changes in the absorption, which were ascribed to the one-electron reduction of **2** to the corresponding radical cation (Fig. 4). In agreement with other related viologens,[27] absorptions at 350–400 nm as well as at 450–500 nm increase upon reduction and new absorptions evolve between 500–650 nm with a maximum centered at 555 nm.

Exfoliation and characterization of graphene/3,10-diazapicenium hybrid systems

With the key features of the *N*,*N*′-dialkylated 3,10-diazapicendiium salt **2** and **3** [28] at hand, we focused on the preparation of the hybrid materials with graphene by adapting a previously reported procedure.[11] Initially, a metastable graphene dispersion (**EG**) was generated in EtOH by ultrasonication for at least 1 h at room temperature and subsequent centrifugation of graphene flakes. This was followed by a stepwise addition of **EG** to a 3 × 10^{-6} M solution of **2** in EtOH affording the hybrid system **EG/2** which was analyzed by steady state absorption spectroscopy, (for details, see ESI†). Our procedure led to exfoliated graphene flakes, which are

stabilized by the diazapicenium cations through π–π interactions. The inherent positive charge of **2** thereby aids in the dispersion of graphene flakes *via* charge repulsion and in that way minimizes their agglomeration in solution. Thus, as the graphene concentration is increased the absorption features of **2** diminish, indicating strong interaction with the basal plane of graphene (Fig. 5). Notably, the peak at about 270 nm, which steadily increases upon adding various aliquots of the graphene dispersion is due to a van Hove singularity in the density of states of graphene.[29] In turn, the fluorescence of **2** is quenched with gradually increasing concentration of **EG** in the dispersion, which is in agreement with previous reports of closely related positively charged exfoliants by Stoddart *et al.* (Fig. 5).[15]

A comprehensive tool to disclose ground state interactions between graphene and **2** is based on Raman spectroscopy. The sample preparation involved drop casting of **EG/2** onto a Si/SiO_2 wafer followed by subsequent drying. To validate our results with **EG/2**, similar experiments were performed with a reference graphene sample, that is, **EG**. **EG** was prepared in analogy to **EG/2** without, however, the addition of **2**. Statistical analyses of the coated wafer were carried out by measuring mappings consisting of 1000 individual spectra recorded upon an excitation wavelength of 532 nm. From 2D/G-ratios on the order of 0.65 as well as a full width at half maximum (FWHM) of the 2D-band of about 70 cm^{-1} we conclude that the majority of the spectra resemble turbostratic graphene flakes.[30] Restacking of the individual graphene flakes during the drying process is a likely rationale for this finding.

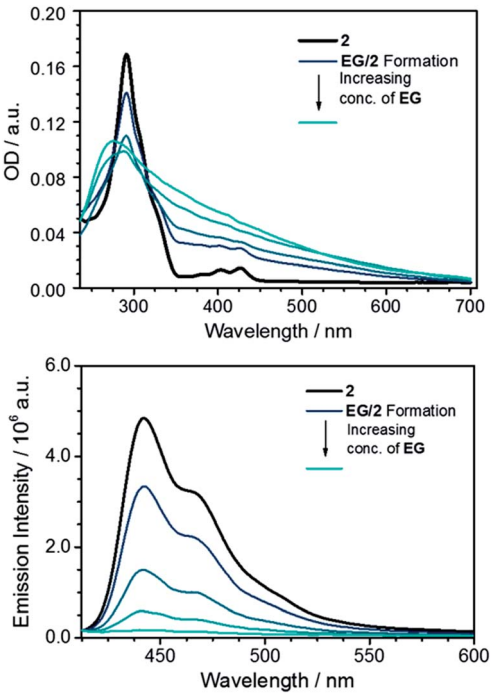

Fig. 5 Top: absorption for clarity **EG/2** spectra shifted in *y*-direction to offset light scattering caused by the graphene/graphite flakes; bottom: fluorescence spectra of **2** (black) and **EG/2** (blue) upon stepwise addition of **EG** in EtOH.

To shed light onto doping effects present in the hybrid material, we focused our attention on the position of the individual Raman bands (Fig. 6). A careful comparison of the histograms regarding the G- and 2D-band positions of **EG/2** and reference **EG** discloses shifts to higher wavenumbers in **EG/2**. Such an upshift is indicative for p-doping of graphene.[31] Such a p-doping is in sound agreement with the electrochemical measurements, in which the low reduction potentials of **2** were documented. In other words, the diazapicenium salt not only acts as a stabilizing agent for exfoliated graphene flakes exploiting the charge repulsion between the cationic scaffolds, but also results in p-doping of the graphene flakes owing to strong electronic coupling in the resulting hybrid material.

To further study the nature of the obtained graphene flakes, atomic force microscopy (AFM) and transmission electron microscopy (TEM) were employed. In typical TEM images of **EG/2**, drop casted from EtOH onto a lacey carbon coated copper grid, few layer graphene with lateral sizes ranging from a few microns as maximum size down to flakes sizes in the nm regime was noted (Fig. 7). Often, the graphene flakes were folded, rolled up, and intertwined. From the height profiles taken from a characteristic AFM image of **EG/2**, which was also used for the Raman measurements, we infer that next to solvent residues and/or some contaminants thin graphene flakes with average heights of 1.9–2.5 nm are present. In combination with the Raman results, these findings demonstrate that the hybrid material consists of turbostratic graphene flakes with a thickness of 5 to 8 layers when probing solid state samples. It is, however, reasonable to assume that the hybrid material consists in the liquid phase of fewer layers due to the repulsive forces introduced from **2**.

Next to steady state measurements, also transient absorption studies were carried out to probe **EG/2**. In the near-infrared region of the spectrum, the usual graphene related bleaching is discernable, for which a lifetime of 0.4 ps was determined. In the visible region of the spectrum, a new transient maximum at

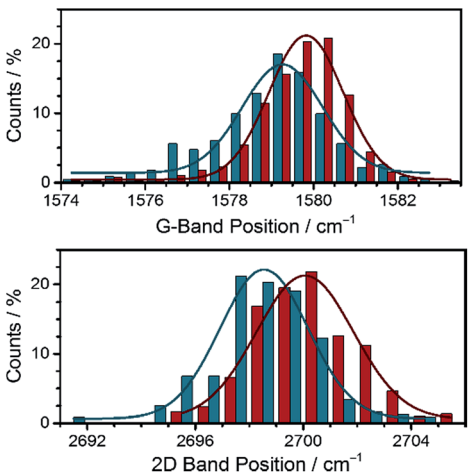

Fig. 6 Statistical analysis of the Raman mapping of reference **EG** (blue bars) as well as of **EG/2** (red bars) displaying the Raman shifts of G-band (top) and 2D-band (bottom). The Gaussian fits serve solely as a guide to the eyes.

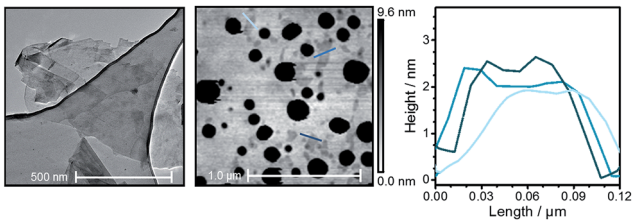

Fig. 7 Left: TEM image of **EG/2** drop casted onto a lacey carbon grid; for the sample typical intertwined and folded multilayered graphene flakes are depicted; middle: AFM picture of **EG/2** drop casted onto a Si/SiO_2 wafer; the black dots constitute residual solvent and/or contaminants; right: height profiles extracted from the AFM image as indicated by the graded blue lines.

595 nm is discernible for **EG/2** (see ESI†). This finding is in sharp contrast to the singlet and triplet excited state features noted for just **2** in EtOH (see Fig. 4). Global analysis of **EG/2** afforded a single evolution associated spectrum with a rather short lifetime of 26 ± 3 ps. Tentatively, we assign this species to that of the charge separated state. As derived from Raman experiments, strong interactions between **EG** and **2** can be regarded as the inception to a doping of **EG** in the ground state. As such, it is reasonable to expect that a partial shift of charge density in the ground state leads to rapid charge separation kinetics in the excited state. Moreover, the comparison of the deconvoluted transient absorption spectrum with the spectroelectrochemical results for **2** confirms that this newly formed transient relates to the one-electron reduced form of **2** (Fig. 8). In comparison to the absorption spectrum of the electrochemically generated radical cation of **2** the maximum is, however, bathochromically shifted by *ca.* 40 nm. A possible rationale for this shift is based on the additional stabilization of the radical cation resulting from electronic coupling with the basal plane of the exfoliated graphene flakes in **EG/2**. Conclusively, the excitation of **EG/2** leads to an electron transfer event from graphene to **2** resulting in a hybrid system consisting of p-doped graphene flakes and radical cations of **2**.

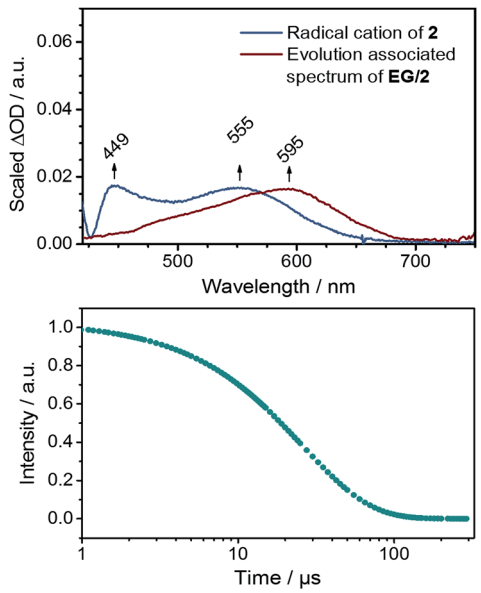

Fig. 8 Top: evolution associated spectrum of **EG/2** together with the differential spectrum from spectroelectrochemical measurements (see Fig. 4). Bottom: corresponding concentration–time profile.

Conclusions

Two novel *N*,*N*′-didodecyl 3,10-diazapicenium salts with bromide and hexafluorophosphate counterions were synthesized as an exfoliant, a stabilizer, and a p-dopant for liquid phase exfoliated graphene. When studied alone, it was demonstrated that the two different counterions of the *N*,*N*′-didodecyl 3,10-diazapicenium salts have only negligible influence on the photophysical and electrochemical properties: both *N*,*N*′-didodecyl 3,10-diazapicenium salts exhibited comparable absorption, fluorescence, and reduction, which were predominantly dictated by the polycyclic π-conjugated scaffold. Complementary spectroelectrochemical investigations with the 3,10-diazapicenium dibromide revealed that their reductions were accompanied by characteristic changes in the absorption features.

The bromide salt was successfully applied to exfoliate graphite and to stabilize the graphene flakes. The resulting hybrids were characterized by an arsenal of steady state and time-resolved spectroscopic as well as microscopic techniques. As such, they corroborate that the ground state of these hybrids is dominated by a shift of charge density from the basal plane of graphene to the positively charged 3,10-diazapicenium: result of this shift is a p-doped graphene. For the excited state, we see an efficient charge transfer from graphene to the positively charged 3,10-diazapicenium. Here, the result is the one-electron reduction of **2** and a hole delocalized on the graphene flakes. Unambiguously, the presence of multilayered turbostratic graphene flakes with modified electronic properties was demonstrated and, hence, the newly synthesized *N*,*N*′-dialkylated 3,10-diazapicenium salts open up highly promising new avenues towards the fabrication of hybrid (nano)graphene materials with electronic properties tailored at will.

Acknowledgements

This work was supported by the Deutsche Forschungsgemeinschaft (DFG) as part of SFB 953 “Synthetic Carbon Allotropes”. The Cluster of Excellence “Engineering of Advanced Materials” (EAM) at FAU Erlangen-Nürnberg, and the Graduate School Molecular Science (GSMS) of FAU Erlangen-Nürnberg are gratefully acknowledged for their generous support. V. C., J. S., and P. J. acknowledge the support from the Czech Science Foundation (grant no. 17-02578S).

Notes and references

1 (*a*) V. Georgakilas, M. Otyepka, A. B. Bourlinos, V. Chandra, N. Kim, K. C. Kemp, P. Hobza, R. Zboril and K. S. Kim, *Chem. Rev.*, 2012, **112**, 6156; (*b*) T. Kuila, S. Bose, A. K. Mishra, P. Khanra, N. H. Kim and J. H. Lee, *Prog. Mater. Sci.*, 2012,

57, 1061; (*c*) A. Ciesielski and P. Samorì, *Adv. Mater.*, 2016, **28**, 6030.

2 (*a*) A. H. Castro Neto, F. Guinea, N. M. R. Peres, K. S. Novoselov and A. K. Geim, *Rev. Mod. Phys.*, 2009, **81**, 109; (*b*) S. Park and R. S. Ruoff, *Nat. Nanotechnol.*, 2009, **4**, 217; (*c*) D. R. Dreyer, R. S. Ruoff and C. W. Bielawski, *Angew. Chem., Int. Ed.*, 2010, **49**, 9336; (*d*) D. A. C. Brownson, D. K. Kampouris and C. E. Banks, *J. Power Sources*, 2011, **196**, 4873.

3 K. S. Novoselov, V. I. Fal'ko, L. Colombo, P. R. Gellert, M. G. Schwab and K. Kim, *Nature*, 2012, **490**, 192.

4 (*a*) L. Jiao, X. Wang, G. Diankov, H. Wang and H. Dai, *Nat. Nanotechnol.*, 2010, **5**, 321; (*b*) X. Li, C. W. Magnuson, A. Venugopal, J. An, J. W. Suk, B. Han, M. Borysiak, W. Cai, A. Velamakanni, Y. Zhu, L. Fu, E. M. Vogel, E. Voelkl, L. Colombo and R. S. Ruoff, *Nano Lett.*, 2010, **10**, 4328.

5 (*a*) F. Li, Y. Bao, J. Chai, Q. Zhang, D. Han and L. Niu, *Langmuir*, 2010, **26**, 12314; (*b*) Y. Zhu, S. Murali, W. Cai, X. Li, J. W. Suk, J. R. Potts and R. S. Ruoff, *Adv. Mater.*, 2010, **22**, 3906; (*c*) I. Levchenko, K. K. Ostrikov, J. Zheng, X. Li, M. Keidar and K. B. K. Teo, *Nanoscale*, 2016, **8**, 10511.

6 (*a*) Y. Si and E. T. Samulski, *Chem. Mater.*, 2008, **20**, 6792; (*b*) M. Lotya, Y. Hernandez, P. J. King, R. J. Smith, V. Nicolosi, L. S. Karlsson, F. M. Blighe, S. De, Z. Wang, I. T. McGovern, G. S. Duesberg and J. N. Coleman, *J. Am. Chem. Soc.*, 2009, **131**, 3611; (*c*) C. Zhang, W. Lv, X. Xie, D. Tang, C. Liu and Q.-H. Yang, *Carbon*, 2013, **62**, 11.

7 D. Kiessling, R. D. Costa, G. Katsukis, J. Malig, F. Lodermeyer, S. Feihl, A. Roth, L. Wibmer, M. Kehrer, M. Volland, P. Wagner, G. G. Wallace, D. L. Officer and D. M. Guldi, *Chem. Sci.*, 2013, **4**, 3085.

8 (*a*) J. Malig, N. Jux, D. Kiessling, J.-J. Cid, P. Vázquez, T. Torres and D. M. Guldi, *Angew. Chem., Int. Ed.*, 2011, **50**, 3561; (*b*) J. Malig, N. Jux and D. M. Guldi, *Acc. Chem. Res.*, 2013, **46**, 53; (*c*) D. M. Guldi and R. D. Costa, *J. Phys. Chem. Lett.*, 2013, **4**, 1489.

9 L. Wibmer, L. M. O. Lourenço, A. Roth, G. Katsukis, M. G. P. M. S. Neves, J. A. S. Cavaleiro, J. P. C. Tomé, T. Torres and D. M. Guldi, *Nanoscale*, 2015, **7**, 5674.

10 J. Malig, A. W. I. Stephenson, P. Wagner, G. G. Wallace, D. L. Officer and D. M. Guldi, *Chem. Commun.*, 2012, **48**, 8745.

11 A. Roth, M.-E. Ragoussi, L. Wibmer, G. Katsukis, G. d. La Torre, T. Torres and D. M. Guldi, *Chem. Sci.*, 2014, **5**, 3432.

12 P. Lauffer, K. V. Emtsev, R. Graupner, T. Seyller and L. Ley, *Phys. Status Solidi B*, 2008, **245**, 2064.

13 X. Dong, D. Fu, W. Fang, Y. Shi, P. Chen and L.-J. Li, *Small*, 2009, **5**, 1422.

14 (*a*) S. S. Sabri, J. Guillemette, A. Guermoune, M. Siaj and T. Szkopek, *Appl. Phys. Lett.*, 2012, **100**, 113106; (*b*) H. B. M. Shashikala, C. I. Nicolas and X.-Q. Wang, *J. Phys. Chem. C*, 2012, **116**, 26102; (*c*) B. Li, A. V. Klekachev, M. Cantoro, C. Huyghebaert, A. Stesmans, I. Asselberghs, S. de Gendt and S. de Feyter, *Nanoscale*, 2013, **5**, 9640; (*d*) T. Hu and I. C. Gerber, *Chem. Phys. Lett.*, 2014, **616–617**, 75; (*e*) L. Zhou, K. Wang, Z. Wu, H. Dong, H. Sun, X. Cheng, H. Zhang, H. Zhou, C. Jia, Q. Jin, H. Mao, J.-L. Coll and J. Zhao, *Langmuir*, 2016, **32**, 12623.

15 S. Sampath, A. N. Basuray, K. J. Hartlieb, T. Aytun, S. I. Stupp and J. F. Stoddart, *Adv. Mater.*, 2013, **25**, 2740.

16 (*a*) V. Calabrese, S. Quici, E. Rossi, E. Cariati, C. Dragonetti, D. Roberto, E. Tordin, F. de Angelis and S. Fantacci, *Chem. Commun.*, 2010, **46**, 8374; (*b*) C. Mitsui, T. Okamoto, H. Matsui, M. Yamagishi, T. Matsushita, J. Soeda, K. Miwa, H. Sato, A. Yamano, T. Uemura and J. Takeya, *Chem. Mater.*, 2013, **25**, 3952; (*c*) Y. Kubozono, K. Hyodo, H. Mori, S. Hamao, H. Goto and Y. Nishihara, *J. Mater. Chem. C*, 2015, **3**, 2413.

17 (*a*) V. Církva and S. Relich, *Curr. Org. Chem.*, 2011, **15**, 248; (*b*) J. Storch, V. Církva and M. B. J. Vokál, Czech Republic Pat., CZ 303997, 2013.

18 3,10-Diazapicene was generously provided by J. Storch and V. Církva from the Institute of Chemical Process Fundamentals of the Czech Academy of Sciences, Prague, Czech Republic.

19 M. Lamberto, E. E. Rastede, J. Decker and F. M. Raymo, *Tetrahedron Lett.*, 2010, **51**, 5618.

20 S. Fanetti, M. Citroni, R. Bini, L. Malavasi, G. A. Artioli and P. Postorino, *J. Chem. Phys.*, 2012, **137**, 224506.

21 T. Bakupog, E. L. Clennan and X. Zhang, *Tetrahedron Lett.*, 2015, **56**, 5591.

22 C. D. Geddes, *Meas. Sci. Technol.*, 2001, **12**, R53.

23 J. Pommerehne, H. Vestweber, W. Guss, R. F. Mahrt, H. Bässler, M. Porsch and J. Daub, *Adv. Mater.*, 1995, **7**, 551.

24 C. L. Bird and A. T. Kuhn, *Chem. Soc. Rev.*, 1981, **10**, 49.

25 G. Jones II, W. R. Jackson, C. Y. Choi and W. R. Bergmark, *J. Phys. Chem.*, 1985, **89**, 294.

26 W. M. Haynes, *CRC Handbook of Chemistry and Physics*, CRC Press, 94th edn, 2013.

27 (*a*) T. M. Bockman and J. K. Kochi, *J. Org. Chem.*, 1990, **55**, 4127; (*b*) C. Reus, M. Stolar, J. Vanderkley, J. Nebauer and T. Baumgartner, *J. Am. Chem. Soc.*, 2015, **137**, 11710.

28 Due to the formation of solvent separated ion pairs in solution and similar electrochemical and photophysical characteristics of **2** and **3**, we expect comparable results for the electronic interactions between the 3,10-diazapicenium dications and graphene; for further information see the ESI.†

29 V. G. Kravets, A. N. Grigorenko, R. R. Nair, P. Blake, S. Anissimova, K. S. Novoselov and A. K. Geim, *Phys. Rev. B: Condens. Matter Mater. Phys.*, 2010, **81**, 155413.

30 A. K. Geim, *Science*, 2009, **324**, 1530.

31 R. Li, Z. Liu, K. Parvez, X. Feng and K. Müllen, *J. Mater. Chem. C*, 2015, **3**, 37.